Libyan Journal of Medical and Applied Sciences LJMAS
Online ISSN: 3006-1113
Volume 3, Issue 3, 2025, Page No: 1-8
Website: https://ljmas.com/index.php/journal/index

Eco-friendly Synthesis of Fe_2O_3 Nanoparticles from B. variegata Extract for Combating Multidrug-Resistant Pathogens

Buthainah Saeeb Saleh [*]
[1] Educational Directorate Anbar, Anbar ,32000, Iraq
[*]Corresponding author: buthaina435@gmail.com

Received: May 30, 2025 Accepted: June 26, 2025 Published: July 01, 2025

Cite this article as: E, S, Saleh. (2025). Eco-friendly Synthesis of Fe_2O_3 Nanoparticles from B. variegata Extract for Combating Multidrug-Resistant Pathogens. Libyan Journal of Medical and Applied Sciences (LJMAS). 2025;3(3):1-8.

Abstract:

This study focused on the biosynthesis of iron nanoparticles using an aqueous extract of Bauhinia Varieties as a reducing agent and stabilizer, followed by an evaluation of their antibacterial activity against several pathogenic bacterial isolates. Given the growing global challenge of antibiotic resistance, particularly in areas such as the Kurdistan Region, the search for effective therapeutic alternatives has become imperative. The nanoparticles were successfully synthesized by reacting ferric nitrate with the plant extract at pHs between 9 and 10 and temperatures between 60 and 80°C. Characterization using Fourier transform infrared spectroscopy (FTIR) confirmed this synthesis by detecting characteristic Fe-O-Fe vibrational bands at wavelengths of 576, 439, and 432 cm^1. Morphological analysis using scanning electron microscopy (SEM) and atomic force microscopy (AFM) confirmed the uniform spherical shape of the nanoparticles, with sizes ranging from 26 to 56nm and a homogeneous distribution. X-ray diffraction (XRD) also confirmed the formation of a pure Fe_2O_3 crystalline structure, with an average crystal size of 28.2nm. In antibacterial tests, the synthesized nanoparticles demonstrated inhibitory activity against all tested strains. The 100% concentration proved most effective against Staphylococcus aureus, showing an inhibition zone diameter of 14.3±1.1 mm. Notably, the 70% concentration showed superior activity against Staphylococcus epidermidis and Escherichia coli, with inhibition zone diameters of 15±1.1 mm and 12.67±1.3 mm, respectively. The nanoparticles reached 83.3% of the efficacy of doxycycline against Staphylococcus epidermidis, and all tested concentrations exceeded 50% of the antibiotic's efficacy against Klebsiella and Escherichia coli. These results confirm the promising potential of Bauhinia-mediated iron nanoparticles as effective antibacterial agents, especially against resistant bacteria. Further research is needed to comprehensively evaluate their toxicity, elucidate their mechanism of action, and explore their potential for synergistic applications with conventional antibiotics in future medical settings.

Keywords: Nanoparticles, Antibacterial Effect, Bauhinia variabilis, Iron Oxide.

تخليق صديق للبيئة لجسيمات نانوية من أكسيد الحديد (Fe_2O_3) من مستخلص بكتيريا B. variegata لمكافحة مسببات الأمراض المقاومة للأدوية المتعددة

بثينة صائب صالح*
[1] مديرية التربية الانبار، الانبار، العراق

الملخص:

ركزت هذه الدراسة على التخليق الحيوي لجسيمات الحديد النانوية باستخدام مستخلص مائي من أصناف بوهينيا كعامل اختزال ومثبت، تبع ذلك تقييم لنشاطها المضاد للبكتيريا ضد العديد من العزلات البكتيرية الممرضة. ونظرًا للتحدي العالمي المتزايد المتمثل في مقاومة المضادات الحيوية، لا سيما في مناطق مثل إقليم كردستان، أصبح البحث عن بدائل علاجية فعالة أمرًا ضروريًا. وقد تم تخليق الجسيمات النانوية بنجاح عن طريق تفاعل نترات الحديديك مع المستخلص النباتي عند درجات حموضة تتراوح بين 9 و10 ودرجات حرارة تتراوح بين 60 و80 درجة مئوية. وقد أكد التوصيف باستخدام مطيافية تحويل فورييه بالأشعة تحت الحمراء (FTIR) هذا التخليق من خلال الكشف عن نطاقات اهتزازية مميزة لـ Fe-O-Fe عند أطوال موجية 576 و439 و432 سم¹. أكد التحليل المورفولوجي باستخدام المجهر الإلكتروني الماسح (SEM) ومجهر القوة الذرية (AFM) الشكل

الكروي الموحد للجسيمات النانوية، بأحجام تتراوح بين 26 و56 نانومترًا وتوزيع متجانس. كما أكد حيود الأشعة السينية (XRD) تكوين بنية بلورية نقية من Fe_2O_3، بمتوسط حجم بلوري يبلغ 28.2 نانومتر. في الاختبارات المضادة للبكتيريا، أظهرت الجسيمات النانوية المُصنّعة نشاطًا مثبطًا ضد جميع السلالات المختبرة. أثبت التركيز 100% فعاليته القصوى ضد المكورات العنقودية الذهبية، حيث أظهر قطر منطقة تثبيط 14.3±1.1 مم. والجدير بالذكر أن التركيز 70% أظهر نشاطًا متفوقًا ضد المكورات العنقودية البشروية والإشريكية القولونية، حيث بلغ قطر منطقة التثبيط 15±1.1 مم و12.67±1.3 مم على التوالي. حققت الجسيمات النانوية 83.3% من فعالية الدوكسيسيكلين ضد المكورات العنقودية البشروية، وتجاوزت جميع التركيزات المختبرة 50% من فعالية المضاد الحيوي ضد الكلبسيلا والإشريكية القولونية. تؤكد هذه النتائج الإمكانات الواعدة لجسيمات الحديد النانوية المُستخدَمة بوساطة البوهينيا كعوامل مضادة للبكتيريا فعالة، وخاصةً ضد البكتيريا المقاومة. هناك حاجة إلى مزيد من البحث لتقييم سميتها بشكل شامل، وتوضيح آلية عملها، واستكشاف إمكاناتها للتطبيقات التآزرية مع المضادات الحيوية التقليدية في البيئات الطبية المستقبلية.

الكلمات المفتاحية: الجسيمات النانوية، التأثير المضاد للبكتيريا، *Bauhinia variabilis* أكسيد الحديد.

Introduction

Antibiotic resistance is one of the most pressing global health crises, posing a fundamental challenge to the effectiveness of modern medical treatments for bacterial infections. In Iraq, particularly within hospitals in Ramadi, Anbar Governorate, alarming reports have documented the spread of multidrug-resistant bacterial strains, including common pathogens such as Staphylococcus aureus and Escherichia coli [1, 2]. This alarming trend is likely a direct result of several complex factors, such as the widespread and indiscriminate use of antibiotics, uncontrolled self-medication, and inadequate adherence to sound infection control protocols.[4 ,3] , In response to this growing challenge, nanotechnology has gained significant momentum as a promising means of combating resistant bacterial strains [5]. Among the most compelling materials in this field are iron nanoparticles, which exhibit potent antimicrobial properties. Their effectiveness is attributed to multiple mechanisms, including the ability to enhance the permeability of bacterial membranes, directly damage cell walls, and generate reactive oxygen species (ROS), which cause severe oxidative stress[6], a sustainable and cost-effective alternative to conventional chemical synthesis methods lies in green synthesis, which uses plant extracts to produce nanostructures [7, 8,9].

Bauhinia variegata, commonly known as the orchid tree, is one such valuable natural resource, valued for its potent medicinal properties; various parts of the plant form the basis of traditional medicinal preparations Despite the well-documented biological activities of plant extracts [9, 10,11], there is still a pressing need for further research into their applications for the manufacture of effective nanoparticles against drug-resistant pathogens, particularly when focusing on sustainable and locally sourced plants [12, 13, 14, 15]. Given this importance, the research aimed to manufacture iron nanoparticles by green synthesis using Bauhinia variegata extract as a reducing agent and stabilizer, and to evaluate the antibacterial activity of the prepared nanoparticles against a variety of Gram-positive and Gram-negative bacterial strains from different clinical sources, including *S. aureus, S. epidermidis*, *E. coli*, and *Klebsiella* spp.

. Material and methods

Synthesis of Iron Nanoparticles

Iron nanoparticles were prepared biosynthetically using B. variegata extract as a reducing and stabilizing agent [16,17]. The method involved adding ferric nitrate solution (0.1 mol/L) to the plant extract, adjusting the pH to 9-10 using sodium hydroxide. The mixture was heated at 60-80°C for 1-2 hours, and a color change to brown was observed, indicating particle formation. After cooling and washing, the particles were oven-dried at 50-60°C. The study determined the optimal reaction conditions at a pH above 10, a temperature of 60-80°C, and a total reaction time of 21 hours.

Characterization of Iron Nanoparticles

To characterize the nanoparticles, multiple analytical techniques were used. Functional groups were examined using FTIR spectroscopy in the 400-4000 cm^{-1} range. To assess the shape and size, a scanning electron microscope (SEM) at 110 kx magnification was used, along with an atomic force microscope (AFM) to obtain three-dimensional images of the surface in non-contact mode. Finally, the crystal structure was determined and the average crystallite size was calculated using X-ray diffraction (XRD) analysis and the Debye-Scherrer equation. All measurements were performed at room temperature (25±2°C) and repeated at least three times to ensure the reliability of the results.

Bacterial Isolates

Bacterial isolates for this study were obtained from the microbiology laboratory of Erbil General Hospital and included Gram-positive *(Staphylococcus aureus and Staphylococcus epidermidis*) and Gram-negative (*Escherichia coli and Klebsiella pneumoniae*) bacteria. The identity of all isolates was confirmed using biochemical tests and a VITEK 2 apparatus, and they were stored in nutrient broth with glycerol at -80°C. Prior to starting the experiments, strains were activated and grown on blood agar and MacConkey agar at 37°C for 24 hours to ensure their purity and viability.

Antibacterial Test

The effectiveness of the nanoparticles prepared from Bohemia against bacterial isolates was evaluated using the disk diffusion method according to the Clinical and Laboratory Standards Institute (CLSI) 2023 standards [18]. Three different concentrations of nanoparticle suspension (50%, 70%, and 100%) were prepared using a base concentration of 10 mg/ml. Their effectiveness was tested against four pathogenic bacteria: Gram-positive *Staphylococcus* aureus and *Staphylococcus* epidermidis, and Gram-negative Escherichia coli and *Klebsiella* spp. Bacterial isolates were prepared by growing them on Mueller-Hinton agar medium, and turbidity was adjusted according to McFarland's 0.5 standard (approximately 1.5×10^8 CFU/ml). The bacterial suspension was spread onto the agar surface using a sterile cotton swab. Sterile paper discs (6 mm diameter) impregnated with different concentrations of nanoparticles were then prepared and placed on the inoculated agar surface. The plates were incubated at 37°C for 24 hours. After incubation, the inhibition zones around the discs were measured in millimeters using a graduated ruler.

Data Analysis

To analyze the data, the study used ImageJ software to assess the size and surface morphology of nanoparticles from microscope images. Statistical analysis was performed using Python to calculate means and standard deviations, and a t-test was performed to compare the effectiveness of different particle concentrations with standard antibiotics, with results considered statistically significant at $p<0.05$. FTIR and XRD spectra were analyzed, and the Debye-Scherrer equation was applied to determine crystallite size. Key results are presented in graphical form.

Results and Discussion

Green Synthesis of Iron Nanoparticles

The characterization results of the nanoparticles prepared using Bohemia—together with each other—show that the particles synthesized in this way had distinct physical and chemical properties. In Figure 1, FTIR analysis revealed several distinct absorption peaks, confirming the success of the biosynthesis process. Bands at 3414 cm^{-1} were due to the aromatic C-H bond elongation mode, H-C-H vibrations at 1382–1427 cm^{-1}, C-O and C-C elongations in the range 1014–1062 cm^{-1}, in addition to the characteristic Fe-O-Fe vibrations at 576, 439, and 432 cm^{-1} (Figure 1).

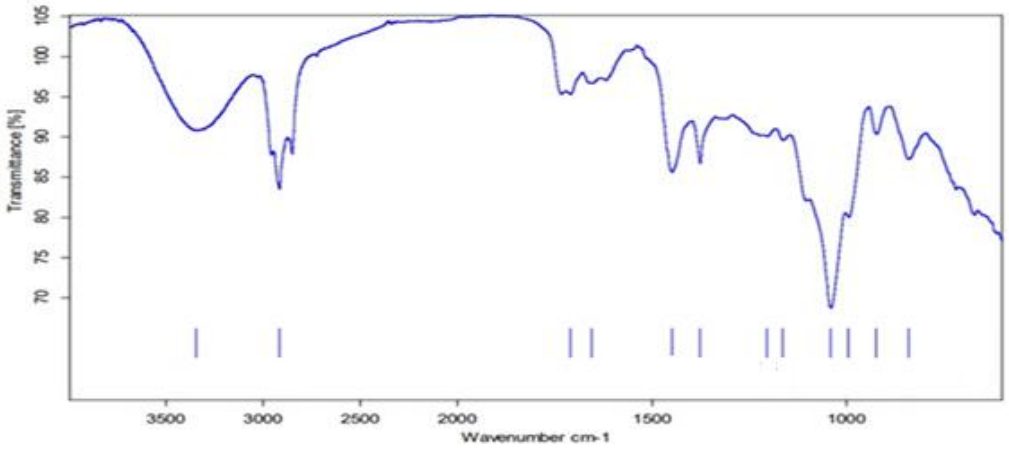

Figure 1. FTIR spectrum analysis of iron nanoparticles prepared using *B. variegata*, showing the characteristic absorption peaks of chemical bonds in the range of 400-4000 cm^{-1}. The main peaks appear at 3414 cm^{-1} (aromatic C-H), 1382-1427 cm^{-1} (H-C-H), and 1014-1062 cm^{-1} (C-O and C-C), with Fe-O-Fe vibrations at 576, 439, and 432 cm^{-1}.

Scanning electron microscope (SEM) images confirmed the regular spherical shapes of the nanoparticles with smooth surfaces and homogeneous size distribution ranging from 26-56 nm (Fig. 2).

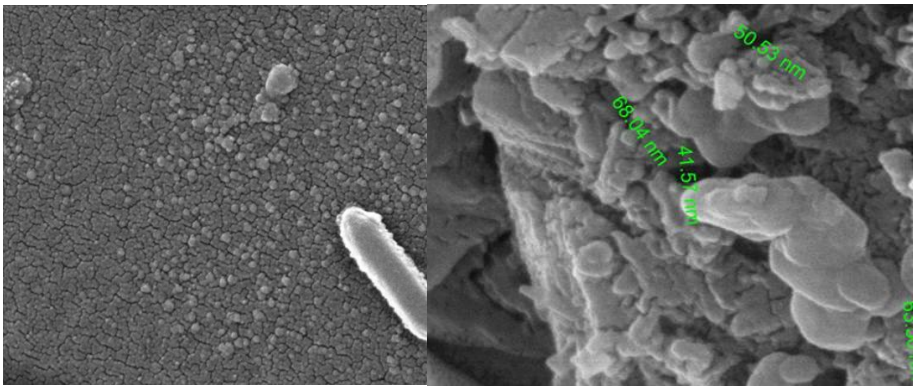

Figure 2. Examination of the sizes and shapes of the biosynthesized iron nanoparticles using Bohemia using a scanning electron microscope (SEM) at a magnification of 110 kx. The images show regular spherical shapes of the nanoparticles with a smooth surface and a size distribution ranging from 26-56 nm.

Atomic energy microscopy (AFM) results also supported these observations, as 2D and 3D images showed a homogeneous distribution of particles with an average diameter of less than 50 nm and a regular surface topography (Figure 3).

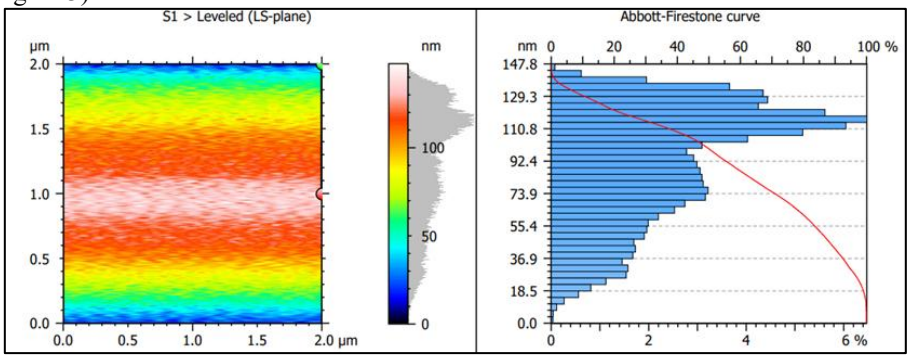

Figure 3. Atomic Energy Microscopy (AFM) images of the prepared iron nanoparticles. The image on the right shows the two-dimensional analysis and the image on the left shows the three-dimensional analysis of the surface topography, it reveals a homogeneous distribution of particles with an average diameter of less than 50 nm and a regular surface topography.

Finally, X-ray diffraction (XRD) analysis confirmed the formation of a pure crystalline structure for Fe_2O_3, with distinct diffraction peaks appearing at 2θ angles of 31.66° and 45.3°, corresponding to crystal distances of 2.85 nm and 1.99 nm, respectively, with an average crystal size of 28.2 nm calculated using the Debye-Scherrer equation (Figure 4).

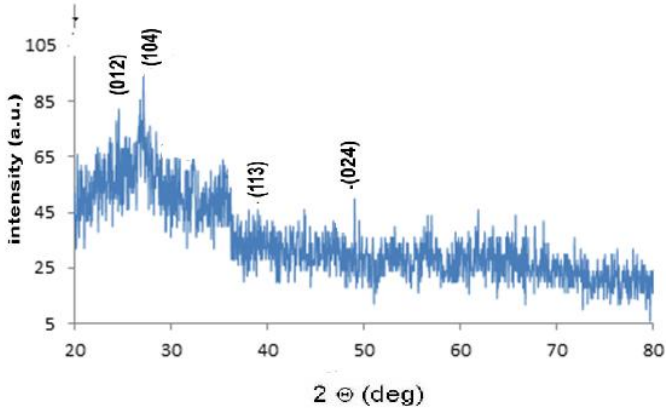

Figure 4. X-ray diffraction (XRD) pattern of the prepared iron nanoparticles, showing characteristic diffraction peaks at 2θ angles equal to 31.66° and 45.3°, corresponding to the crystal distances of 2.85 nm and 1.99 nm, respectively, confirming the formation of a pure crystal structure of Fe_2O_3 with an average crystal size of 28.2 nm.

Effect of nano-iron on pathogenic bacteria

The results of the antibacterial activity test of iron nanoparticles prepared using Bohemia showed varying efficacy against the tested bacterial strains (Figure 5). For S. aureus, the nanoparticles showed increasing inhibitory activity with increasing concentration, with inhibition zones of 13±1.1, 14±0, and 14.3±1.1 mm for concentrations of 50%, 70%, and 100%, respectively, compared to 30±1 mm for clindamycin ($p<0.001$). For S. epidermidis, the highest inhibitory activity was observed at the 70% concentration (15±1.1 mm), compared to the other two concentrations and 18±2 mm for doxycycline ($p=0.05$). As for E. coli, the nanoparticles showed moderate activity with the best effect at 70% concentration (12.67±1.3 mM) compared to chloramphenicol (20±2 mM). Finally, the results against Klebsiella spp. showed similar activity across different concentrations (13.67, 11.67±1.2, and 12.33±1.3 mM) compared to meropenem (20±2 mM).

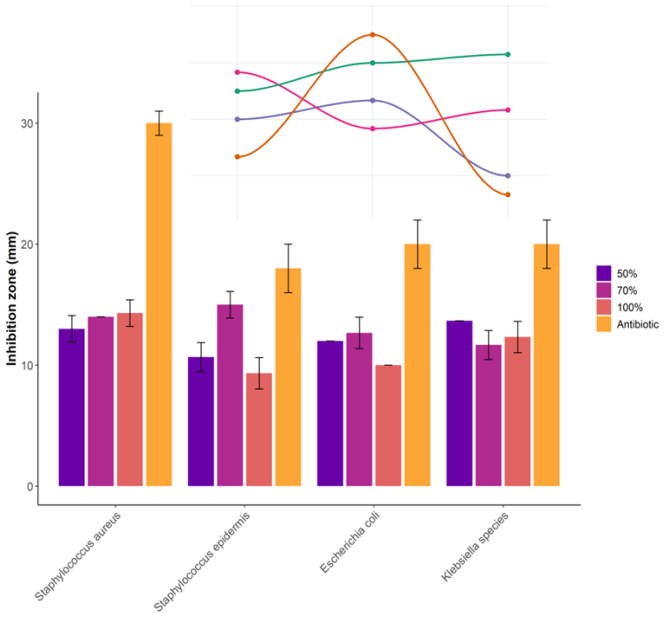

Figure 5. The antibacterial effect of iron nanoparticles against different bacterial species according to different concentrations and compared to the effect of the standard antibiotic.

Fourier transform infrared (FTIR) spectroscopy confirmed the successful biosynthesis of iron nanoparticles. The spectra showed distinct absorption bands at 576, 439, and 432 cm^{-1}, attributed to the vibrations of Fe-O-Fe bonds, consistent with previous studies on iron oxide nanoparticles [19,20,21]. The spectrum also revealed the presence of functional groups in the Bauhinia extract, such as O-H and C-O groups, which played a vital role in reducing iron ions and capping and stabilizing the nanoparticles, consistent with documented green synthesis mechanisms [22,23]. These results confirm that the plant extract was not only a reducing agent but also contributed to stabilizing the particles and imparting antimicrobial properties [24]. Regarding the results of scanning electron microscopy (SEM) and atomic force microscopy (AFM) analysis, morphological and topographical characteristics of iron nanoparticles prepared using plant extracts, SEM images revealed a regular spherical shape of the particles with a smooth surface and a size distribution ranging from 26-56 nm, which is consistent with what Alamilla-Martínez et al. (2019) reported about the spherical shape of biosynthesized nanoparticles [25]. The AFM examination results supported these observations through 2D and 3D images that showed a homogeneous distribution of particles with an average diameter of less than 50 nm. This homogeneous distribution can be attributed to the effective role of plant as a stabilizing agent. Shaik et al. (2018) indicated that increasing the concentration of natural and plant extracts typically results in a reduced nanoparticle size and improved distribution [26]. These results are also consistent with the study by Stozhko et al. (2019), which demonstrated that the antioxidant activity of plant extracts significantly affects the synthesis kinetics, size, and stability of nanoparticles [27]. AFM results showed the absence of significant agglomerations, which is consistent with the study by Velgosova et al. (2024), which indicated the role of phytochemical compounds in plant extracts in preventing particle agglomeration [28]. It was also observed that the iron nanoparticles prepared in this study fall within the ideal size range for bioapplications (10–80 nm), according to Tarafdar and Raliya, enhancing their

potential as antimicrobial materials [29]. X-ray diffraction (XRD) analysis confirmed the successful synthesis of iron oxide nanoparticles with a regular crystalline structure. Sharp, distinct peaks at 2θ angles of 31.66° and 45.3° indicated the formation of a pure hematite (α-Fe_2O_3) phase, consistent with the results of previous studies [30]. Using the Debye-Scherrer equation, the average crystal size was calculated to be 28.2 nm, which is ideal for biological applications and consistent with other studies [31]. The broad peaks indicate the small size of the particles, while their sharpness confirms the purity of the crystals [32]. These results confirm the effectiveness of the plant extract in producing highly crystalline nanoparticles suitable for medical uses. The results of the current study show that iron nanoparticles prepared using bohemia possess antibacterial activity against both Gram-positive and Gram-negative bacteria, albeit to varying degrees. These results are consistent with those of Behera et al. (2012), who indicated that iron oxide nanoparticles exhibit moderate antibacterial activity against a wide range of pathogenic bacteria [33]. An effect that increased with increasing concentration was also observed, with different concentrations (50%, 70%, 100%) showing varying efficacy against the tested bacterial strains. This is consistent with the study by Gupta et al. (2020), which confirmed that the effectiveness of metal nanoparticles is highly dependent on the concentration used [34]. It is noted that the highest inhibitory activity against Staphylococcus aureus was at the 100% concentration (14.3±1.1 mM), while the 70% concentration was most effective against Staphylococcus aureus (15±1.1 mM) and Escherichia coli (12.67±1.3 mM). These results are consistent with what Muthiah et al. (2016) reported on the effect of nanoparticle concentration on their physicochemical properties, as it can affect the dissolution rate and cluster formation, and thus their biological activity [35]. In the same context, Shoudho et al. (2024) indicated that the physicochemical properties of nanoparticles significantly affect their antibacterial activity by influencing the production of reactive oxygen species (ROS), which disrupt bacterial cells.[36]

The effectiveness of some concentrations, especially the 100% concentration, against S. epidermidis and E. coli, may be attributed to the phenomenon of "self-toxicity" or the formation of nanoparticle aggregates at high concentrations, which reduces the effective surface area and thus affects its antibacterial activity. This is consistent with the study by Merrifield et al. (2017) which indicated that the concentration of nanoparticles significantly affects their fate and transformation in complex media.[37]

When comparing the effectiveness of nanoparticles to standard antibiotics, the efficacy was generally lower, but the inhibition rate exceeded 50% of the antibiotic's efficacy in several cases, particularly against S. epidermidis at a concentration of 70%. This is consistent with the study by Gudkov et al. (2021), which indicated the potential use of iron oxide nanoparticles as a new generation of antimicrobial agents [38]. The mechanism of action by which the prepared nanoparticles potentially affect the pathogenesis may involve several pathways, as indicated by Slavin et al. (2017), including the production of reactive oxygen species and free radicals, the release of iron ions, interaction with bacterial cell membranes, and disruption of cellular processes [39]. Huang et al. (2023) also demonstrated that nanoparticles can enter and accumulate within bacterial cells, leading to increased ROS levels, lipid peroxidation, DNA damage, and cell death.[42,41,40] .

Conclusions

This research successfully demonstrated the eco-friendly green synthesis of iron nanoparticles utilizing an extract from the *Bauhinia* plant. Advanced characterization techniques, including FTIR, SEM, AFM, and XRD, confirmed that the synthesized particles are spherical, fall within a size range of 26-56 nm, and possess a pure crystalline Fe_2O_3 structure. The synthesized nanoparticles exhibited effective antimicrobial activity against both Gram-positive and Gram-negative bacteria. The 70% concentration proved most effective against *Staphylococcus epidermidis* and *E. coli*, while the 100% concentration showed the highest potency against *Staphylococcus aureus*. Notably, the nanoparticles' efficacy against *S. epidermidis* reached 83.3% of the activity of the antibiotic Doxycycline at the 70% concentration. Furthermore, their effectiveness surpassed 50% of the standard antibiotics' efficacy against both *Klebsiella spp.* and *E. coli*.

Disclaimer

The article has not been previously presented or published, and is not part of a thesis project.

Conflict of Interest

There are no financial, personal, or professional conflicts of interest to declare.

References

1. Kazaal MA, Hamad WA, Atiya WH, Saeed BJ, Abd-Alsatar AN. Impact of antibiotic resistance on sustainable development goals. AIP Conf. Proc. 2023; 020016. doi: 10.1063/5.0137246.
2. Al-Fahad DK, Alpofead JA, Chawsheen MA, Al-Naqshbandi AA, Abas AT. Surveillance of antimicrobial resistance in Iraq. ARO-THE Sci. J. KOYA Univ. 2024; 12:179–93. doi: 10.14500/aro.11689.

3. Darwish DA, Abdelmalek S, Dayyih WA, Hamadi S. Awareness of antibiotic use and antimicrobial resistance in the Iraqi community in Jordan. J. Infect. Dev. Ctries. 2014; 8:616–23. doi: 10.3855/jidc.4086.
4. Tan LY, Sin LT, Bee ST, Ratnam CT, Woo KK, Tee TT, Rahmat AR. A review of antimicrobial fabric containing nanostructures metal-based compound. J. Vinyl Addit. Technol. 2019; 25:E3–E27. doi: 10.1002/vnl.21606.
5. de Toledo L de AS, Rosseto HC, Bruschi ML. Iron oxide magnetic nanoparticles as antimicrobials for therapeutics. Pharm. Dev. Technol. 2018; 23:316–23. doi: 10.1080/10837450.2017.1337793.
6. Baien SH, Seele J, Henneck T, Freibrodt C, Szura G, Moubasher H, Nau R, Brogden G, Mörgelin M, Singh M, Kietzmann M, von Köckritz-Blickwede M, de Buhr N. Antimicrobial and Immunomodulatory Effect of Gum Arabic on Human and Bovine Granulocytes Against Staphylococcus aureus and Escherichia coli. Front. Immunol. 2019; 10:3119. doi: 10.3389/fimmu.2019.03119.
7. Aslam B, Wang W, Arshad MI, Khurshid M, Muzammil S, Rasool MH, Nisar MA, Alvi RF, Aslam MA, Qamar MU, Salamat MKF, Baloch Z. Antibiotic resistance: a rundown of a global crisis. Infect. Drug Resist. 2018; 11:1645–58. doi: 10.2147/IDR.S173867.
8. Batool F, Iqbal MS, Khan SUD, Khan J, Ahmed B, Qadir MI. Biologically synthesized iron nanoparticles (FeNPs) from Phoenix dactylifera have anti-bacterial activities. Sci. Rep. 2021; 11:22132.
9. Al-Dahmoshi HOM, Al-Khafaji NSK, Al-Allak MHO. Antibiotic resistance among Iraqi local E. coli isolates. E. Coli Infect. - Importance Early Diagnosis Effic. Treat. 2020. doi: 10.5772/intechopen.92107.
10. WHO. Fact sheets on SDG: health targets and Antimicrobial Resistance. 2017.
11. Abbas ZK, Owaid MN. Prevalence of Antibiotics Resistance in the Isolated Bacteria from Bronchial Washing Fluids in Ramadi Teaching Hospital, Iraq. Gazi Med. J. 2021; 32. doi: 10.12996/gmj.2021.83.
12. Mutlk ST. Isolation and characterization of MDR- Klebsiella pneumonia phage from Euphrates River in Al-Anbar city. Int. J. Health Sci. (Qassim). 2022; 6:5115–23. doi: 10.53730/ijhs.v6nS2.6208.
13. Abbas D, Al.janabi A, N. W. Bacterial Infection in Male Infertility in Al-Anbar Province West Of Iraq. Egypt. Acad. J. Biol. Sci. G. Microbiol. 2019. doi: 10.21608/eajbsg.2019.36319.
14. Abid N, Hamad E, Ibrahim M, Abid H. Antibacterial and antibiofilm activities of taxifolin against vancomycin-resistant S. aureus (VRSA). Baghdad J. Biochem. Appl. Biol. Sci. 2022; 3:262–72. doi: 10.47419/bjbabs.v3i04.126.
15. Factors impacting knoweldge, practice and attitude about antibacterial and its resistance by cross sectional study in Iraq. J. Pharm. Negat. Results. 2022; 13. doi: 10.47750/pnr.2022.13.S01.68.
16. Garcia BS. The Antimicrobial Therapy of the Future: Combating Resistances. J. Infect. Dis. Ther. 2014; 02. doi: 10.4172/2332-0877.1000146.
17. Almawla SOG, Rajab NA, Edan AE, Mohammed AT. Uropathogenic Bacterial Detection and Surveillance of Antimicrobial Resistance Pattern in Urine Specimens Referred to Al anbar Province. South East. Eur. J. Public Heal. 2024; 26:492–506. doi: 10.70135/seejph.vi.1090.
18. Sharqi HM, Hassan OM, Obaid AS. Investigation of the antibiotic-resistant ESKAPE pathogens in Ramadi hospitals, Iraq. Indian J. Forensic Med. Toxicol. 2021; 15:3306–13. doi: 10.37506/ijfmt.v15i4.17219.
19. Antibiotics Misuse and Factors Leading to Its' Abuse in Kurdistan Region. J. Heal. Med. Nurs. 2016. doi: 10.7176/JHMN/24-2016-05.
20. Al-Jumaili AA, Ahmed KK. A review of antibiotic misuse and bacterial resistance in Iraq. East. Mediterr. Heal. J. 2024; 30:663–70. doi: 10.26719/2024.30.10.663.
21. Helmy YA, Taha-Abdelaziz K, Hawwas HAE-H, Ghosh S, AlKafaas SS, Moawad MMM, Saied EM, Kassem II, Mawad AMM. Antimicrobial Resistance and Recent Alternatives to Antibiotics for the Control of Bacterial Pathogens with an Emphasis on Foodborne Pathogens. Antibiotics. 2023; 12:274. doi: 10.3390/antibiotics12020274.
22. Mdarhri HA, Benmessaoud R, Yacoubi H, Seffar L, Assimi HG, Hamam M, Boussettine R, Filali-Ansari N, Lahlou FA, Diawara I, Ennaji MM, Kettani-Halabi M. Alternatives Therapeutic Approaches to Conventional Antibiotics: Advantages, Limitations and Potential Application in Medicine. Antibiotics. 2022; 11:1826. doi: 10.3390/antibiotics11121826.
23. Kharisov BI, Dias HVR, Kharissova OV, Jiménez-Pérez VM, Pérez BO, Flores BM. Iron-containing nanomaterials: synthesis, properties, and environmental applications. RSC Adv. 2012; 2:9325. doi: 10.1039/c2ra20812a.

24. Taghizadeh S-M, Berenjian A, Zare M, Ebrahiminezhad A. New perspectives on iron-based nanostructures. Processes. 2020; 8:1128. doi: 10.3390/pr8091128.
25. Alamilla-Martínez DG, Rojas-Avelizapa NG, Domínguez-López I, Pool H, Gómez-Ramírez M. Biosynthesis of iron nanoparticles (FeNPs) by Alternaria alternata MVSS-AH-5. Mex. J. Biotechnol. 2019; 4:1–14. doi: 10.29267/mxjb.2019.4.4.1.
26. Shaik M, Khan M, Kuniyil M, Al-Warthan A, Alkhathlan H, Siddiqui M, Shaik J, Ahamed A, Mahmood A, Khan M, Adil S. Plant-Extract-Assisted Green Synthesis of Silver Nanoparticles Using Origanum vulgare L. Extract and Their Microbicidal Activities. Sustainability. 2018; 10:913. doi: 10.3390/su10040913.
27. Stozhko NY, Bukharinova MA, Khamzina EI, Tarasov AV, Vidrevich MB, Brainina KZ. The Effect of the Antioxidant Activity of Plant Extracts on the Properties of Iron Nanoparticles. Nanomaterials. 2019; 9:1655. doi: 10.3390/nano91201655.
28. Velgosova O, Dolinská S, Podolská H, Mačák L, Čižmárová E. Impact of Plant Extract Phytochemicals on the Synthesis of Silver Nanoparticles. Materials (Basel). 2024; 17:2252. doi: 10.3390/ma17102252.
29. Yamada Y, Nishida N. Iron-based Nanoparticles and Their Mössbauer Spectra. Radioisotopes. 2019; 68:125–43. doi: 10.3769/radioisotopes.68.125.
30. Pattanayak M, Nayak PL. Ecofriendly green synthesis of iron nano particles from various plants and spices extract. Int. J. Plant, Anim. Environ. Sci. 2013.
31. Barman B. Process of Synthesis and Analysis of Nanoparticles Recovered by Magnetic Methods. Am. J. Phys. Chem. 2024; 13:91–7. doi: 10.11648/j.ajpc.20241304.13.
32. Alphandéry E. Iron oxide nanoparticles for therapeutic applications. Drug Discov. Today. 2020; 25:141–9. doi: 10.1016/j.drudis.2019.09.020.
33. Behera SS, Patra JK, Pramanik K, Panda N, Thatoi H. Characterization and Evaluation of Antibacterial Activities of Chemically Synthesized Iron Oxide Nanoparticles. World J. Nano Sci. Eng. 2012; 02:196–200. doi: 10.4236/wjnse.2012.24026.
34. Gupta V, Kant V, Sharma AK, Sharma M. Comparative assessment of antibacterial efficacy for cobalt nanoparticles, bulk cobalt and standard antibiotics: A concentration dependant study. Nanosyst. Physics, Chem. Math. 2020; 11:78–85. doi: 10.17586/2220-8054-2020-11-1-78-85.
35. Muthiah M, Park I-K, Cho C-S. Surface modification of iron oxide nanoparticles by biocompatible polymers for tissue imaging and targeting. Biotechnol. Adv. 2013; 31:1224–36. doi: 10.1016/j.biotechadv.2013.03.005.
36. Shoudho KN, Uddin S, Rumon MMH, Shakil MS. Influence of Physicochemical Properties of Iron Oxide Nanoparticles on Their Antibacterial Activity. ACS Omega. 2024; 9:33303–34. doi: 10.1021/acsomega.4c02822.
37. Elshemy M. Iron Oxide Nanoparticles Versus Ferrous Sulfate In Treatment of Iron Deficiency Anemia In Rats. Egypt. J. Vet. Sci. 2018; 49:103–9. doi: 10.21608/ejvs.2018.3855.1039.
38. Gudkov SV, Burmistrov DE, Serov DA, Rebezov MB, Semenova AA, Lisitsyn AB. Do Iron Oxide Nanoparticles Have Significant Antibacterial Properties? Antibiotics. 2021; 10:884. doi: 10.3390/antibiotics10070884.
39. Slavin YN, Asnis J, Häfeli UO, Bach H. Metal nanoparticles: understanding the mechanisms behind antibacterial activity. J. Nanobiotechnology. 2017; 15:65. doi: 10.1186/s12951-017-0308-z.
40. Huang C, Duan M, Shi Y, Liu H, Zhang P, Zuo Y, Yan L, Xu Y, Niu Y. Insights into the antibacterial mechanism of iron doped carbon dots. J. Colloid Interface Sci. 2023; 645:933–42. doi: 10.1016/j.jcis.2023.04.149.
41. Skłodowski K, Chmielewska-Deptuła SJ, Piktel E, Wolak P, Wollny T, Bucki R. Metallic Nanosystems in the Development of Antimicrobial Strategies with High Antimicrobial Activity and High Biocompatibility. Int. J. Mol. Sci. 2023; 24:2104. doi: 10.3390/ijms24032104.
42. Fardood ST, Ramazani A, Joo SW. Eco-friendly Synthesis of Magnesium Oxide Nanoparticles using Arabic Gum. Q. J. Appl. Chem. Res. 2018; 12:8–15